

MAJOR PAPER

Combining the Tumor Contact Length and Apparent Diffusion Coefficient Better Predicts Extraprostatic Extension of Prostate Cancer with Capsular Abutment: A 3 Tesla MR Imaging Study

Koichi Ito¹, Emiko Chiba¹, Noriko Oyama-Manabe^{1*}, Satoshi Washino²,
Osamu Manabe¹, Tomoaki Miyagawa², Kohei Hamamoto¹, Masahiro Hiruta³,
Keisuke Tanno¹, and Hiroshi Shinmoto⁴

Purpose: To assess the diagnostic performance of the tumor contact length (TCL) and apparent diffusion coefficient (ADC) for predicting extraprostatic extension (EPE) of prostate cancer with capsular abutment (CA).

Methods: Ninety-three patients with biopsy-proven prostate cancer underwent 3-Tesla MRI, including diffusion-weighted imaging (b value = 0, 2000 s/mm²) and radical prostatectomy. Two experienced radiologists, blinded to the clinicopathological data, retrospectively assessed the presence of CA on T2-weighted imaging (T2WI). TCL on T2WI and ADC values were measured on detecting CA in prostate cancer. We used the receiver operating characteristic curves to assess the diagnostic performance of TCL and ADC values for predicting EPE.

Results: CA was present in 58 prostate cancers among 93 patients. The cut-off value for TCL was 6.9 mm, which yielded an area under the curve (AUC) of 0.75. This corresponded to a sensitivity, specificity, and accuracy of 84.2%, 61.5%, and 69.0%, respectively. The cut-off value for ADC was 0.63×10^{-3} mm²/s, which yielded an AUC of 0.76. This, in turn, corresponded to a sensitivity, specificity, and accuracy of 84.2%, 59.0%, and 67.2%, respectively. The combined cut-off value of TCL and ADC yielded an AUC of 0.82. The specificity (84.6%) and accuracy (81.0%) of the combined value were superior to their individual values ($P < 0.05$).

Conclusion: A combination of TCL and ADC values provided high specificity and accuracy for detecting EPE of prostatic cancer with CA.

Keywords: prostate cancer, capsular abutment, extraprostatic extension, tumor contact length, apparent diffusion coefficient

Introduction

Extraprostatic extension (EPE) is one of the most important prognostic factors for prostate cancer.¹ Therefore, EPE

prediction facilitates therapeutic decision-making and prognosis estimation in patients undergoing radical prostatectomy. Some nomograms, including prostate-specific antigen (PSA), digital rectal examination, and pathological information from biopsy, have been used to predict EPE.²

MRI using T2-weighted imaging (T2WI) has been increasingly used for the accurate diagnosis of EPE.³ Imaging findings suggestive of EPE are capsular irregularity, neurovascular bundle thickening, bulging, loss of the capsule, and measurable extracapsular disease.⁴ According to recent studies, 36–60% of prostate cancers are positive for capsular abutment (CA). The latter is classified as a low suspicious MR finding (score 1) in the European Society of Urogenital Radiology (ESUR) prostate MR guidelines 2012 for diagnosing EPE.^{4–6} However, 14–39% of prostate cancers with CA are finally diagnosed with EPE after radical prostatectomy.^{5,7} MRI prediction of EPE is generally difficult in prostate cancer with CA. Tumor contact length (TCL), defined as the length of a lesion in contact

¹Department of Radiology, Jichi Medical University Saitama Medical Center, Saitama, Saitama, Japan

²Department of Urology, Jichi Medical University Saitama Medical Center, Saitama, Saitama, Japan

³Department of Pathology, Jichi Medical University Saitama Medical Center, Saitama, Saitama, Japan

⁴Department of Radiology, National Defense Medical College, Tokorozawa, Saitama, Japan

*Corresponding author: Department of Radiology, Jichi Medical University Saitama Medical Center, 1-847, Amanumacho, Omiya-ku, Saitama, Saitama 330-8503, Japan. Phone: +81-48-647-2111, Fax: +81-48-648-5188, E-mail: norikomanabe@jichi.ac.jp



This work is licensed under a Creative Commons Attribution-NonCommercial-NoDerivatives International License.

with the prostatic capsule, could act as a reliable marker. In addition, TCL greater than 10 mm may indicate EPE.^{5,8} However, the TCL would not be a sufficient predictor of prostate cancer with CA. Therefore, MRI prediction of EPE of prostate cancer with CA needs to be investigated. The diagnostic ability of EPE in prostate cancers with CA was improved on adding the apparent diffusion coefficient (ADC).⁹

Few studies have examined the diagnostic performances of TCL and ADC values at 3-Tesla (T) MRI for predicting EPE of prostate cancer with CA. Thus, we aimed to assess their diagnostic performances for the prediction of EPE of prostate cancer with CA.

Materials and Methods

Participants

This retrospective study was approved by our institutional review board and the requirement for obtaining informed consent from the patients was waived. Ninety-four consecutive patients with biopsy-proved prostate cancer underwent prostate MRI with a 3-T system between June 2014 and July 2019. All patients underwent MR examination before biopsy. They underwent MRI, followed by radical prostatectomy within 180 days. We excluded one patient for a marked artifact on diffusion-weighted imaging (DWI) related to a distortion from gas in the rectum. This exclusion provided a final cohort of 93 patients. None of them were treated with hormonal therapy before the operation. The summary of patient characteristics can be found in Table 1.

MRI technique

All images were obtained under fasting conditions using a 3-T MR scanner (Vantage Titan 3-T; Canon Medical Systems, Tochigi, Japan) with a 16-channel phased-array coil (Atlas SPEEDER Body; Canon Medical Systems), combined with a 40-channel phased-array coil (Atlas SPEEDER Spine). The protocol for prostate MRI included the following steps: axial T1-weighted fast spin-echo imaging, axial and sagittal T2-weighted fast spin-echo imaging, and axial DWI. Axial DWI was performed using a multi-section spin-echo, single-shot echo-planar imaging sequence. Following the acquisition at b values of 0 and 2000 s/mm², the motion-probing gradient pulses were applied sequentially along three orthogonal orientations to acquire the DWI values. We reconstructed the ADC maps by calculating the ADC in each pixel of each slice. In addition, the ADC values were calculated for a pair of b values of 0 and 2000 s/mm². The locations of axial T1-weighted imaging (T1WI), axial T2WI, and axial DWI were the same. Table 2 summarises the technical parameters of all MRI sequences assessed in this study. Despite obtaining dynamic contrast-enhanced images, we could not assess them as a part of this study.

Table 1 Summary of characteristics of patient cohort

Characteristics	Value
No. of patients	93
Age (years)	67.9 (51–78)
Prostate volume (ml)	46.4 (14.3–127)
Pretreatment serum PSA (ng/ml)	12.7 (2.7–121.6)
Gleason score on biopsy	
5 + 4	2 (2.2)
4 + 5	19 (20.4)
4 + 4	5 (5.4)
4 + 3	22 (23.7)
3 + 5	3 (3.2)
3 + 4	37 (39.8)
3 + 3	5 (5.4)
The final Gleason score on radical prostatectomy	
5 + 4	3 (3.4)
4 + 5	25 (27.3)
4 + 4	4 (4.5)
4 + 3	16 (18.2)
3 + 5	2 (2.3)
3 + 4	41 (42)
3 + 3	2 (2.3)

Continuous variables are expressed as median (range) values, and categorical variables are expressed as number (%) of patients. PSA, prostate-specific antigen.

Histopathologic analysis

We determined the reference standard for tumor localization and EPE of prostate cancer using the step-section histologic slices from radical prostatectomy. The prostatectomy specimens were sliced from the apex to the base at 3- to 5-mm intervals in a plane, perpendicular to the prostatic urethra. The distal portion of the apex and the proximal portion of the base were amputated and sliced sagittally to assess the resection margin. We processed all slices uniformly and submitted them entirely. Following the routine hematoxylin–eosin staining, all pathologic specimens were blindly reviewed without MRI findings. The tumor location, presence, and location of EPE were pathologically recorded. EPE was histopathologically defined as the presence of cancer cells beyond the prostatic capsular margin, extending into the periprostatic adipose tissue.¹⁰

Image interpretation and data analysis

Figure 1 summarises the process of image interpretation and data analysis. The MR images were evaluated using

Table 2 Technical parameters of MRI sequences assessed in this study

Parameter	T1WI	T2WI	T2WI	DWI
Acquisition mode	FSE	FSE	FSE	FSE
Plane	Axial	Axial	Sagittal	Axial
TR/TE (ms)	500/10	4000/12	4000/12	2000/87
Echo train length	2	27	27	27
Flip angle (°)	120	120	120	90
b values (s/mm ²)	NA	NA	NA	0 and 2000
Field of View (cm)	23 × 23	23 × 23	23 × 23	23 × 23
Matrix Size	256 × 352	256 × 384	256 × 384	128 × 112
No. of excitation	1	1	1	3
Slices thickness (mm)	3.5	3.5	3.5	3.5
Slice gap (mm)	0.7	0.7	0.7	0.7
Parallel Imaging Factor	1.4	1.2	NA	1.5
Scan Time	2 min 42 s	2 min 16 s	2 min 32 s	3 min 37 s

DWI, diffusion-weighted imaging; EPI, echo-planar imaging; FSE, fast spin-echo; NA, not applicable; T1WI, T1-weighted Image; T2WI, T2-weighted Image; TE, echo time; TR, repetition time.

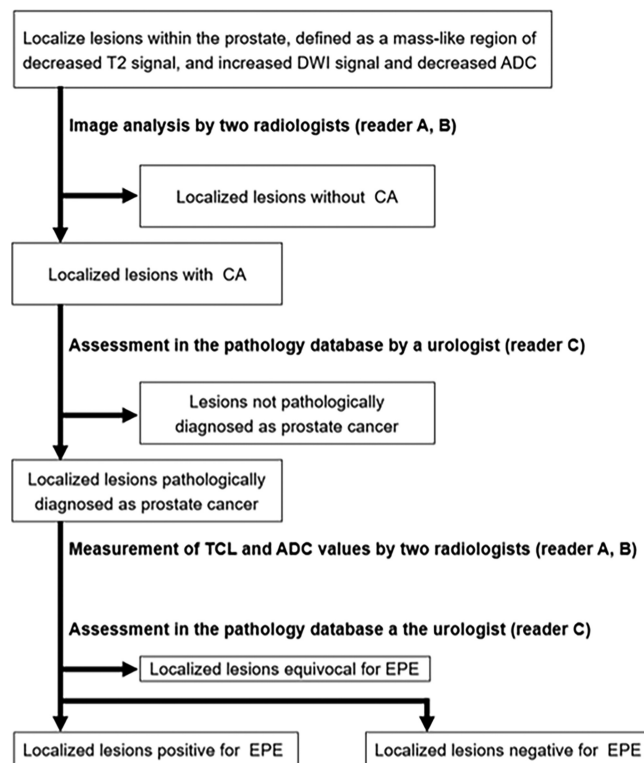


Fig. 1 Image interpretation and data analysis. A total of 175 magnetic resonance imaging localized lesions with suspected prostate cancer were retrospectively enrolled. After excluding prostate cancers without CA and pathologically equivocal for EPE ($n = 2$), we studied the remaining 58 prostate cancers with CA. We classified 58 prostate cancers into two groups, namely EPE positive ($n = 19$) and EPE negative ($n = 39$). ADC, apparent diffusion coefficient; CA, capsular abutment; DWI, diffusion weighted imaging; EPE, extraprostatic extension; TCL, tumor contact length.

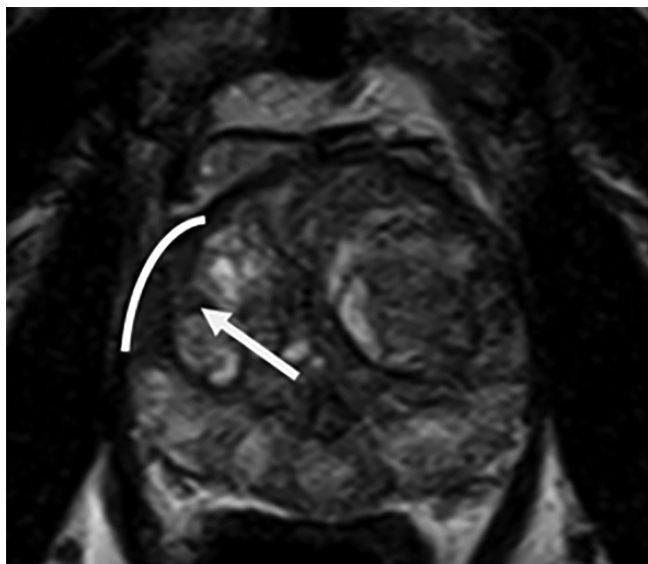


Fig. 2 TCL measurement. A representative case of a 69-year-old man with prostate cancer. The lesion with capsular abutment (arrow) is in the right middle region in the peripheral zone on axial T2-weighted imaging. The white line shows the TCL, defined as the contour length of the lesion in contact with prostatic capsule. TCL, tumor contact length.

picture archiving and communication systems (PACS) viewer (Synapse EX-V; Fujifilm, Tokyo, Japan). Two board certified radiologists (E.C., reader A, and K.I., reader B), with 8 and 9 years of experience, independently interpreted the prostate MR imaging. They were aware that all patients had biopsy-proven prostate cancer. Nonetheless, they were blinded to clinical and pathologic data. They reviewed all images for each patient to localize the lesions within the prostate, defined as a mass-like region of decreased T2 signal and decreased ADC.⁸ T1WI was used to delineate the outline of the gland.³

They assessed the presence of CA for each localized lesion.⁶ CA was marked absent when the lesions showed the following findings: 1) location away from the prostatic capsule (highly unlikely of EPE); 2) asymmetric invasion of the neurovascular bundles, a bulging prostatic contour, an irregular or spiculated margin, an obliteration of the recto-prostatic angle, and a breach of the capsule with evidence of direct tumor extension or bladder wall invasion (suggestive of EPE).³ They discussed their findings to reach a consensus during disagreement.

An experienced urologist (W.S., reader C), acquainted with MRI and pathology of prostate cancer, reviewed the localized lesions on MRI. He assessed the pathology database to determine the presence of prostate cancer on MRI. The radiologists (readers A and B) independently measured the TCL and ADC values of pathologically localized lesions. They were blinded to the presence or absence of EPE. The TCL of the localized lesions, with the largest surface of contact with the prostatic capsule seen on axial T2WI, was measured in millimeters, using the digitalized line meter

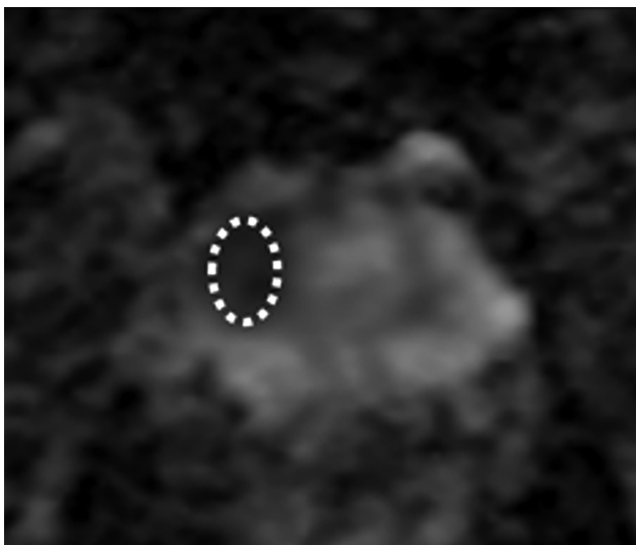


Fig. 3 ADC value measurement. A representative case of a 71-year-old man with prostate cancer. The localized lesion shows a high signal on axial diffusion-weighted imaging with b values of 2000 s/mm². It corresponds to the low-signal area on the axial ADC map. An oval region of interest was chosen to be as large as possible within the low ADC area. Great care was taken to include only the inner aspect of the lesion to reduce the partial volume effects. ADC, apparent diffusion coefficient.

function. TCL was measured using a curve ruler tool (Fig. 2). The ROI placement technique was used for the ADC maps on the PACS monitor to measure ADC. Each ROI was circular or oval and was chosen to be as large as possible within the low ADC area. The radiologists took great care to only include the inner aspect of the lesion to reduce partial volume effects (Fig. 3). Furthermore, the ADC value of the lesion was measured on the same slice of the measured TCL value on axial T2WI. This was followed by calculating the average values of each TCL and ADC, measured by each radiologist.

The urologist (reader C) then referred to the records in the pathology database to confirm the presence of EPE in the localized lesions. He was blinded to the aforementioned values.

Statistical analysis

We compared the TCL and ADC values of the lesion with CA between those positive and negative for EPE using the unpaired Student's t-test. We used the receiver operating characteristic (ROC) curves to assess the diagnostic performance of the above-mentioned values for predicting EPE of prostate cancer with CA. The area under the ROC curve facilitated the establishment of the optimal cut-off points. We assessed the diagnostic performance by calculating the AUC.

We designed the logistics regression analysis model using the values of TCL and ADC, and the EPE as the independent and dependent variables, respectively. The

Table 3 Diagnostic performance for the detection of EPE in TCL values, ADC values, and combined TCL and ADC values

	TCL values	ADC values	Combined TCL and ADC values
Cut-off Value	6.9 mm	$0.63 \times 10^{-3} \text{ mm}^2/\text{s}$	$6.9 \text{ mm} + 0.63 \times 10^{-3} \text{ mm}^2/\text{s}$
AUC (95% CI)	0.75 (0.61–0.88)	0.76 (0.64–0.89)	0.82 (0.70–0.94)
Sensitivity (%)	84.2 (16/19)	84.2 (16/19)	73.7 (14/19)
Specificity (%)	61.5 (24/39)	59.0 (23/39)	84.6 (33/39)
PPV (%)	51.6 (16/31)	50.0 (16/32)	70.0 (14/20)
NPV (%)	88.9 (24/27)	88.5 (23/26)	86.8 (33/38)
Accuracy (%)	69.0 (40/58)	67.2 (39/58)	81.0 (47/58)

Data represent percentages, with values used to calculate these percentages provided in parentheses. ADC, apparent diffusion coefficient; AUC, area under the curve; CI, confidence interval; EPE, extraprostatic extension; NPV, negative predictive value; PPV, positive predictive value; TCL, tumor contact length.

ROC analysis enabled the assessment of the operative performance of the prediction model for EPE. If the lesion met the cut-off of both TCL and ADC values, it was considered positive for EPE. If the lesion met the cut-off of either TCL or ADC values, it was considered negative for EPE.

We used the McNemar test to compare the sensitivity, specificity, and accuracy between the combined and individual values. In addition, we performed the χ^2 test to compare between the ROC curves.

We evaluated the interobserver agreement on the presence of CA between the radiologists using weighted κ statistics. The κ values were interpreted as follows: < 0.20 indicated poor agreement, $0.21\text{--}0.40$ indicated fair agreement, $0.41\text{--}0.60$ indicated moderate agreement, $0.61\text{--}0.80$ indicated good agreement, and ≥ 0.80 indicated excellent agreement.¹¹ The inter-operator reproducibility for the TCL and ADC measurement between readers A and B was assessed using intra-class correlation coefficients (ICC).

All statistical analyses were performed using JMP Pro 14.0.0 software program (SAS Institute, Cary, NC, USA). A P value < 0.05 was considered to be statistically significant.

Results

Lesion characteristics

CA was defined as present in 68 lesions of all MRI localized lesions. Of the 68 localized lesions with CA, 60 were pathologically diagnosed as prostate cancer (Gleason scores ≥ 7). Of 60 lesions pathologically diagnosed as prostate cancer, 18 lesions were located in the transition zone and 42 lesions were located in the peripheral zone. Figure 1 shows the numbers of localized lesions, with or without CA. Sixty localized lesions were designated as positive ($n = 19$), negative ($n = 39$), or equivocal ($n = 2$) for EPE. Finally, we analyzed 58 lesions designated after 2 lesions designated as equivocal were excluded.

Interobserver agreement between the radiologists

A visual analysis of the interobserver agreement between the radiologists on the assessment of the presence of CA demonstrated a κ value of 0.678 (range, 0.564–0.792), thus indicating good agreement. The ICC for the TCL and ADC measurement was 0.873 and 0.949, respectively. Both values showed high inter-operator reproducibility with ICCs over 0.80.

Assessment of EPE

The TCL and ADC values were significantly different between the two groups of lesions. The mean TCL values were 10.8 ± 5.6 and 6.8 ± 3.1 (mm) for those positive and negative for EPE, respectively ($P < 0.001$). The mean ADC values ($\times 10^{-3} \text{ mm}^2/\text{s}$) were 0.55 ± 0.10 and 0.68 ± 0.16 for lesions positive and negative for EPE, respectively ($P = 0.001$).

Table 3 summarises the diagnostic performances for the detection of EPE in TCL, ADC, and combined values.

The cut-off for TCL was 6.9 mm, which yielded an AUC of 0.75, corresponding to a sensitivity, specificity, and accuracy of 84.2%, 61.5%, and 69.0%, respectively. In contrast, the cut-off for ADC value was $0.63 \times 10^{-3} \text{ mm}^2/\text{s}$, which yielded an AUC of 0.76, corresponding to a sensitivity, specificity, and accuracy of 84.2%, 59.0%, and 67.2%, respectively. The combined cut-off values of TCL (6.9 mm) and ADC ($0.63 \times 10^{-3} \text{ mm}^2/\text{s}$) yielded an AUC of 0.82. This corresponded to a sensitivity, specificity, and accuracy of 73.7%, 84.6%, and 81.0%, respectively.

The specificity and accuracy of the combined values were superior to those of TCL alone ($P = 0.003$ and $P = 0.035$, respectively). Moreover, they were superior to those of ADC alone ($P = 0.002$ and $P = 0.021$, respectively).

The comparisons of the ROC curves of the EPE predictors using TCL, ADC, and combined values are shown in Fig. 4. The AUC of the combined values was higher than those of TCL and ADC. Nonetheless, the difference was statistically insignificant ($P = 0.195$ and $P = 0.214$, respectively).

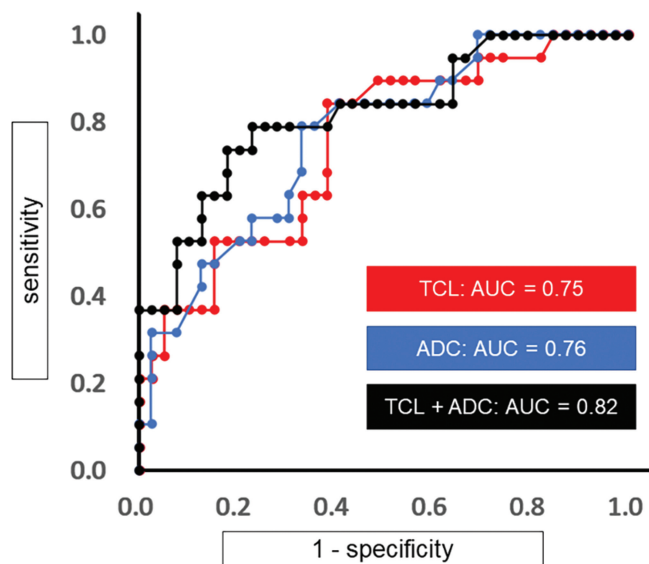


Fig. 4 ROC curves of the EPE predictors. The AUC in ROC analysis for prediction of EPE using each TCL or ADC was 0.75 or 0.76, respectively. On combining TCL and ADC, the AUC increased to 0.82. ADC, apparent diffusion coefficient; AUC, area under the curve; EPE, extraprostatic extension; ROC, receiver operating characteristic; TCL, tumor contact length.

When conducting the binominal logistics regression analysis, we confirmed that the cut-off for 6.9 mm TCL is an EPE predictor with statistically significant results (OR = 1.2, $P = 0.04$). In addition, the cut-off for $0.63 \times 10^{-3} \text{ mm}^2/\text{s}$ ADC predicts EPE with statistically significant results (OR = 1.0×10^{-3} , $P = 0.03$).

Discussion

When using the cut-off value for TCL 6.9 mm, and for ADC $0.63 \times 10^{-3} \text{ mm}^2/\text{s}$ to predict EPE, each value showed high sensitivity for predicting EPE of prostate cancer with CA. In addition, the combined cut-off value yielded a better AUC of 0.82, showing high specificity and accuracy.

Microscopic EPE has been reported in 29% of the patients who underwent radical prostatectomy.¹² It is imperative to know if there is EPE (Stage 3a or more) for selecting an appropriate treatment strategy in patients with prostate cancer who undergo radical prostatectomy.¹³

Clinical staging, based on digital rectal examination, PSA, and transrectal US findings, sometimes resulted in understaging (59%).¹⁴ Prostate MRI using T2WI is considered as a useful imaging modality for diagnosing EPE.

However, the diagnosis of EPE with T2WI alone is more difficult, particularly in prostate cancer with CA. Furthermore, the diagnostic criterion that uses T2WI for EPE is not well established. According to the study conducted by Kido et al., the rate of an accurate diagnosis of EPE with T2WI alone was 64% (7/11 patients).⁹ Nonetheless, the overall accuracy increased to 91% (10/11 patients) with an additional ADC cut-off value ($0.72 \times 10^{-3} \text{ mm}^2/\text{s}$).

Specificity is more important than sensitivity for determining EPE to prevent the exclusion of patients from potentially curative treatment.¹⁵ Thus, a combination of

TCL and ADC values could be more reliable for diagnosing EPE than the values alone.

Table 4 contains a summary of the previous studies for predicting EPE with TCL/ADC values. The study by Granja et al. at 1.5 T used a combination of both values.¹⁶ Granja et al. measured the TCL and ADC values of prostate cancers with any of the following findings: abutment, irregularity, neurovascular bundle thickening, bulge, or loss of capsule on T2WI.⁶ In contrast, we measured the TCL and ADC values of prostate cancers with CA, which corresponded to abutment at 3-T MRI.

The cut-off value for TCL in this study was lower than that of the studies conducted by Baco et al. and Granja et al.^{16,17} However, it was similar to that used by Rosenkrantz et al.⁸ According to the MRI grading system proposed by Mehrlivand et al., TCL greater than 1.5 cm (EPE Grade 1) suggests pathological EPE.¹⁸ These differences may result from several factors, such as the zonal origin (transition or peripheral, anterior or posterior) of the tumor and clinical setting.^{19,20}

The cut-off value for ADC in our study was lower than that of the studies conducted by Woo et al. and Granja et al.^{7,16} This may be attributed to the ADC values obtained with different b values: high b value ($2000 \text{ s}/\text{mm}^2$) in our study and standard b values ($800, 1000 \text{ s}/\text{mm}^2$) in the studies conducted by Woo et al. and Granja et al. At relatively low b values, signal intensity in DWI is dominated by fast-diffusing water molecules that are mostly extracellular, while, at higher b values, signal intensity is largely attributable to slow-diffusing water molecules that are either bound to macromolecules or confined within the cell membrane. The decrease in ADC observed at higher b-value DWI in this study may be affected by the higher sensitivity to slow-diffusion water molecules.²¹

Our study had several limitations. First, the retrospective design might have introduced selection bias. Secondly, the technical parameters of MRI sequences are different from those based on Prostate Imaging Reporting and Data System

Table 4. A review table of previous studies for the prediction of EPE in prostate cancer with the measurement of the TCL/ADC values

Study	Magnet Strength	No. of Patients	Parameters	Cut-off value (b value) [#]	Diagnostic performance (SEN, SPE, AUC)
Our study	3T	93	TCL/ADC	TCL: 6.9 mm	TCL: 84%, 62%, 0.75
				ADC: $0.63 \times 10^{-3} \text{ mm}^2/\text{s}$	ADC: 84%, 59%, 0.76
				(b value = 0, 2000 s/mm ²)	TCL+ADC: 74%, 85%, 0.82
Granja ¹⁵	1.5T	92	TCL/ADC	TCL: 17.5 mm	TCL: 91%, 57%, 0.74
				ADC: $0.87 \times 10^{-3} \text{ mm}^2/\text{s}$	ADC: 83%, 61%, 0.72
				(b value = 200, 800 s/mm ²)	TCL+ADC: 77%, 61%, 0.77
Rosenkrantz ⁸	3T	90	TCL	TCL: 6 mm	TCL: 80–89%, 73–75%, 0.81
Baco ¹⁶	1.5T	111	TCL	TCL: 20 mm	TCL: 79%, 85%, 0.88
Woo ⁷	3T	117	ADC	ADC: $0.89 \times 10^{-3} \text{ mm}^2/\text{s}$	ADC: 92%, 55%, 0.76
Kido ^{*9}	3T	43	ADC	(b value = 0, 1000 s/mm ²)	
				ADC: $0.72 \times 10^{-3} \text{ mm}^2/\text{s}$	ADC: 78%, 96%, NA
				(b value = 0, 2000 s/mm ²)	(Accuracy: 91%)

[#] Pair of b values for calculation of ADC values. * Sensitivity, specificity, and accuracy were evaluated with combined ADC values and T2WI findings suggestive of EPE. While sensitivity and specificity were evaluated in all patients (43 patients), accuracy was evaluated in prostate cancers with capsular abutment (11 patients). ADC, apparent diffusion coefficient; AUC, area under the curve; EPE, extraprostatic extension; NA, not available; SEN, sensitivity; SPE, specificity; T2WI, T2-weighted imaging; TCL, tumor contact length.

version 2 (PI-RADS v2; American College of Radiology, Reston, VA, USA, European Society of Urogenital Radiology, Wien, Austria, and AdMeTech Foundation, Boston, MA, USA). We used ADC values obtained with high b value (2000 s/mm²), not same as the recommended b values of PI-RADS v2 (750-900 s/mm²).³ The relevance of the ADC values obtained with high b value can be attributed to their usefulness in predicting tumor aggressiveness, EPE, and surgical margin status in prostate cancer.^{9,22,23} Despite the slice thickness (3.5 mm) being greater than the recommended thickness of PI-RADS v2 (3 mm),³ this difference is unlikely to have a significant effect on TCL values. Thirdly, the ADC values might differ under the influence of the MR scanner type, magnetic field strength, and b values. Therefore, it is necessary for each institution to determine the optimal ADC cut-off value. This can be associated with the failure in adapting our ADC cut-off value to other institutions. Fourthly, ambiguous marginal ROI could not be used on the PACS monitor. In all lesions with CA, each ROI was circular or oval and was chosen to be as large as possible within the lesion. We took great care to include only the inner aspect of the lesion to reduce partial volume effects.

Conclusion

In conclusion, the TCL and ADC values were good predictors of EPE of prostate cancer with CA. A combination of these values provided higher diagnostic specificity and accuracy. Therefore, they might act as good markers for the optimal treatment strategy of prostate cancer with CA.

Conflicts of Interest

Noriko Oyama-Manabe Activities related to the present article: disclosed no relevant relationships. Activities not related to the present article: consultant for Canon Medical Systems; grant from the Japan Society for the Promotion of Science (JSPS) KAKENHI; payment for lectures from Daiichi-Sankyo, Philips Medical Systems, Eisai, Bayer Healthcare, and Canon Medical Systems Other activities: disclosed no relevant relationships.

The other authors have no conflicts of interest to declare.

References

- Ball MW, Partin AW, Epstein JI. Extent of extraprostatic extension independently influences biochemical recurrence-free survival: evidence for further pT3 subclassification. *Urology* 2015; 85:161–164.
- Tosoian JJ, Chappidi M, Feng Z, et al. Prediction of pathological stage based on clinical stage, serum prostate-specific antigen, and biopsy Gleason score: Partin Tables in the contemporary era. *BJU Int* 2017; 119:676–683.
- Weinreb JC, Barentsz JO, Choyke PL, et al. PI-RADS prostate imaging - Reporting and data system: 2015, Version 2. *Eur Urol* 2016; 69:16–40.
- Boesen L, Chabanova E, Løgager V, et al. Prostate cancer staging with extracapsular extension risk scoring using multiparametric MRI: a correlation with histopathology. *Eur Radiol* 2015; 25:1776–1785.
- Matsuoka Y, Ishioka J, Tanaka H, et al. Impact of the prostate imaging reporting and data system, Version 2, on MRI

- diagnosis for extracapsular extension of prostate cancer. *AJR Am J Roentgenol* 2017; 209:W76–W84.
6. Barentsz JO, Richenberg J, Clements R, et al.; European society of urogenital radiology. ESUR prostate MR guidelines 2012. *Eur Radiol* 2012; 22: 746–757.
 7. Woo S, Cho JY, Kim SY, et al. Extracapsular extension in prostate cancer: added value of diffusion-weighted MRI in patients with equivocal findings on T2-weighted imaging. *AJR Am J Roentgenol* 2015; 204:W168–175.
 8. Rosenkrantz AB, Shanbhogue AK, Wang A, et al. Length of capsular contact for diagnosing extraprostatic extension on prostate MRI: Assessment at an optimal threshold. *J Magn Reson Imaging* 2016; 43:990–997.
 9. Kido A, Tamada T, Sone T, et al. Incremental value of high b value diffusion-weighted magnetic resonance imaging at 3-T for prediction of extracapsular extension in patients with prostate cancer: preliminary experience. *Radiol Med* 2017; 122:228–238.
 10. Ohori M, Kattan M, Scardino PT, et al. Radical prostatectomy for carcinoma of the prostate. *Mod Pathol* 2004; 17:349–359.
 11. Landis JR, Koch GG. The measurement of observer agreement for categorical data. *Biometrics* 1977; 33:159–174.
 12. Budäus L, Spethmann J, Isbarn H, et al. Inverse stage migration in patients undergoing radical prostatectomy: results of 8916 European patients treated within the last decade. *BJU Int* 2011; 108:1256–1261.
 13. Hoedemaeker RF, Vis AN Van Der Kwast TH. Staging prostate cancer. *Microsc Res Tech* 2000; 51:423–429.
 14. Bostwick DG. Staging prostate cancer—1997: current methods and limitations. *Eur Urol* 1997; 32 Suppl 3:2–14.
 15. Fütterer JJ, Engelbrecht MR, Huisman HJ, et al. Staging prostate cancer with dynamic contrast-enhanced endorectal MR imaging prior to radical prostatectomy: experienced versus less experienced readers. *Radiology* 2005; 237:541–549.
 16. Granja MF, Pedraza CM, Flórez DC, et al. Predicting extracapsular involvement in prostate cancer through the tumor contact length and the apparent diffusion coefficient. *Radiologia* 2017; 59:313–320.
 17. Baco E, Rud E, Vlatkovic L, et al. Predictive value of magnetic resonance imaging determined tumor contact length for extracapsular extension of prostate cancer. *J Urol* 2015; 193:466–472.
 18. Mehralivand S, Shih JH, Harmon S, et al. A grading system for the assessment of risk of extraprostatic extension of prostate cancer at multiparametric MRI. *Radiology* 2019; 290:709–719.
 19. Rud E, Diep L, Baco E. A prospective study evaluating indirect MRI-signs for the prediction of extraprostatic disease in patients with prostate cancer: tumor volume, tumor contact length and tumor apparent diffusion coefficient. *World J Urol* 2018; 36:629–637.
 20. Matsumoto K, Akita H, Narita K, et al. Prediction of extraprostatic extension by MRI tumor contact length: difference between anterior and posterior prostate cancer. *Prostate Cancer Prostatic Dis* 2019; 22:539–545.
 21. Kitajima K, Takahashi S, Ueno Y, et al. Do apparent diffusion coefficient (ADC) values obtained using high b-values with a 3-T MRI correlate better than a transrectal ultrasound (TRUS)-guided biopsy with true Gleason scores obtained from radical prostatectomy specimens for patients with prostate cancer? *Eur J Radiol* 2013; 82:1219–1226.
 22. Kitajima K, Takahashi S, Ueno Y, et al. Clinical utility of apparent diffusion coefficient values obtained using high b-value when diagnosing prostate cancer using 3 tesla MRI: comparison between ultra-high b-value (2000 s/mm²) and standard high b-value (1000 s/mm²). *J Magn Reson Imaging* 2012; 36:198–205.
 23. Tamada T, Sone T, Kanomata N, et al. Value of preoperative 3T multiparametric MRI for surgical margin status in patients with prostate cancer. *J Magn Reson Imaging* 2016; 44:584–593.